Diffusion Model for a Convective Layer. Part I: Numerical Simulation of Convective Boundary Layer

WEN-YIH SUN AND CHIAO-ZEN CHANG

Department of Geosciences, Purdue University, West Lafayette, IN 47907

(Manuscript received 1 July 1985, in final form 5 April 1986)

ABSTRACT

A simple turbulence model is used to study the moist convective boundary layer, in which a prognostic equation is applied to calculate the turbulent kinetic energy E. An observational length scale of the vertical velocity component, l, is used in the mixed layer, while a length scale associated with gravity waves is applied in the stable layer. The eddy coefficient is proportional to $\sqrt{E}l$. This model simulates well the temperature, mixing ratio and mean wind observed in the Wangara experiments. The turbulent kinetic energy and eddy fluxes generated are also in good agreement with those observed, as well as with those obtained from other more complicated models. Furthermore, the parameterization and results generated are used in a pollution model, which will be presented in Part II of this study.

1. Introduction

In recent years, several authors have developed higher-order turbulence closure schemes in order to study the convective boundary layer. One of the most important contributions is Deardorff's (1974a,b) three-dimensional numerical experiment, in which a major portion of the turbulence was explicitly calculated and subgrid-scale turbulence was modeled by a second-order closure approximation. Since Deardorff's scheme requires a very small resolution in all three spatial dimensions and time, it needs a very large amount of computing time and requires a huge amount of central memory. Hence his subgrid-scale turbulence parameterization is very difficult to apply in a mesoscale model, in which the width of the horizontal domain can vary from a few tens to a thousand kilometers with coarse resolutions in both vertical and horizontal directions. Therefore, Mellor and Yamada (1974), Wyngaard and Coté (1974), Zeman and Lumley (1976), André et al. (1978) and many others have worked on the higher-order ensemble-average turbulence schemes. Generally, these one-dimensional schemes require much less computing time compared to Deardorff's three-dimensional model. Nevertheless, the equations of a one-dimensional model are quite complicated, even with approximations suitable for a horizontally homogeneous boundary layer. For instance, all of the second moments and the dissipation term are integrated from partial differential equations in Wyngaard and Coté's (1974) model. The second-order model developed by Zeman and Lumley (1976) requires 12 prognostic differential equations for the higher-order moments, in addition to the differential equations for the first moments in a dry atmosphere, and the third-order model for a moist planetary boundary proposed by André et al. (1976a, 1978) consists of 33 prognostic equations for the turbulence fields.

Mellor and Yamada (1974) presented an analysis that systematically simplifies the second-order closure model (i.e., the level-4 model in Mellor and Yamada's terminology) into the level-3 model. The level-3 model uses only two prognostic partial differential equations and a set of linear algebraic equations for solving the turbulence variables in a dry convective boundary layer.

Mellor and Yamada's level-3 model has been applied by Yamada and Mellor (1975) to simulate the diurnal variations of the planetary boundary layer observed during the Wangara experiment. The gross behavior of the simulated boundary layer is comparable to observations. However, the depth of the simulated mixed layer is consistently underestimated; the intensity of the simulated convection is considerably weaker than those observed or simulated by other models. Hence, Sun and Ogura (1980) modified Mellor and Yamada's turbulence scheme by incorporating the formulae for the third-order moments and pressure terms proposed by Zeman and Lumley (1976). Sun and Ogura (1980) also introduced the turbulence length scale, which depends upon the stratification of the atmosphere, in contrast to that used by Mellor and Yamada (1974) or Deardorff (1974a,b). It is noted that in Sun and Ogura's model, five prognostic differential equations were integrated in order to obtain the turbulent kinetic energy, temperature variance, temperature–humidity covariance, and heat and moisture fluxes, in addition to the differential equations for the mean variables. The pres-

sure and transport terms proposed by Zeman and Lumley (1976), which were used in Sun and Ogura's model, are also much more complicated than those proposed by Mellor and Yamada. Although Sun and Ogura's results compare more favorably to the Wangara data than Yamada and Mellor's (1975) simulations, Sun and Ogura's turbulence scheme is more difficult to apply in two- or three-dimensional mesoscale models than the Mellor and Yamada level-3 turbulence parameterization. It is noted that Mellor and Yamada's level-3 model has also been modified and applied by Enger (1983a,b) to simulate the Wangara data as well as the pollution distribution in a convective layer.

Deardorff (1980) has simplified his second-order turbulence scheme (Deardorff, 1974a,b) by assuming that the eddy-coefficient relations are valid for eddy fluxes and that the eddy coefficient is proportional to the square root of the turbulent kinetic energy. Hence, only one prognostic equation is needed for the turbulent kinetic energy in order to solve the eddy fluxes of heat, moisture and momentum. Although Deardorff's (1980) scheme is designed to calculate subgrid-scale turbulence, his basic equations are very similar to those of the Mellor and Yamada (1977) level-2.5 ensemble-average turbulence scheme, although the latter scheme has more complicated formulae for the length scale and eddy coefficients.

Instead of developing a new theory or providing any different physical explanations for the complicated phenomena in a convective boundary layer, we are going to introduce an ensemble-average turbulence model that is simple enough to be applied in a mesoscale pollution model; it is also capable of predicting realistic results for the wind, temperature and moisture fields, as well as the eddy transports. Our equations are similar to those of Deardorff (1980), except that the observational peak wavelength for the vertical velocity component obtained by Caughey and Palmer (1979) is introduced as the turbulence length scale in the convective layer. It is noted that this model cannot simulate temperature variance, temperature–humidity covariance, and the third-moments as obtained by Zeman and Lumley (1976), André et al. (1978), Sun and Ogura (1980) and others. However, the calculated temperature, wind, moisture, heat and moisture fluxes, and some other turbulence variables are comparable to those produced by the higher-order turbulence schemes as well as to those observed. Because of the simplicity of this scheme, it can be incorporated easily into an air pollution model, which will be presented in Part II of this study (Sun and Chang, 1986). This turbulence scheme has also been used in a three-dimensional mesoscale model developed at Purdue University (Sun and Hsu, 1985) to study the cold air outbreak over the Kuroshio Current and to simulate the mesoscale convection along the dryline, which will be discussed in other papers.

2. Governing equations

The fundamental equations for the mean variables in an adiabatic, quasi-horizontally homogeneous flow are

$$\partial U/\partial t = fV - fV_g + \partial(\overline{-uw})/\partial z, \tag{1}$$

$$\partial V/\partial t = -fU + fU_g + \partial(\overline{-vw})/\partial z, \tag{2}$$

$$\partial \Theta/\partial t = \partial(\overline{-w\theta})/\partial z, \tag{3}$$

$$\partial Q/\partial t = \partial(\overline{-wq})/\partial z. \tag{4}$$

Here (U, V) are the mean horizontal velocities in the x (eastward) and y (northward) directions; Θ is the virtual potential temperature, which is defined as $\Theta = \Theta_d(1 + 0.61Q)$, where Q is the mixing ratio of water vapor; Θ_d is the potential temperature for dry air; $f = -0.826 \times 10^{-4}\ \mathrm{s}^{-1}$ is the Coriolis parameter at Hay, Australia (34°30′S, 144°56′E); $\overline{uw}$, $\overline{vw}$ are components of the Reynolds stress tensor in the x- and y-directions, respectively; and $\overline{w\theta}$ and $\overline{wq}$ are the components of turbulent heat flux and moisture flux, respectively. Here the pressure gradients are substituted by (fU_g, fV_g), because in the Wangara dataset, pressure gradients were provided in the form of geostrophic wind profiles according to

$$fU_g = -1/\rho(\partial p/\partial y), \tag{5a}$$

$$fV_g = 1/\rho(\partial p/\partial x). \tag{5b}$$

The equation for the time rate of change of turbulent kinetic energy is

$$\partial E/\partial t = (g/\Theta)\overline{w\theta} - \overline{uw}\partial U/\partial z - \overline{vw}\partial V/\partial z - \partial[\overline{w(E' + p'/\rho)}]/\partial z - \epsilon \tag{6}$$

where $E' = 0.5(u^2 + v^2 + w^2)$ is the turbulent kinetic energy, and $E = \overline{E'}$ is the ensemble average. The first term on the right-hand side represents the buoyant production, the second and third terms represent the wind shear production, the fourth term represents the transport term, and ϵ is the rate of dissipation due to small eddies. As mentioned previously, Deardorff's (1980) eddy-coefficient relations are employed for fluxes of semiconservative quantities, and the eddy coefficients are made proportional to the square root of the turbulent kinetic energy. The eddy fluxes are parameterized by

$$\overline{uw} = -K_m(\partial U/\partial z), \tag{7}$$

$$\overline{vw} = -K_m(\partial V/\partial z), \tag{8}$$

$$\overline{w\theta} = -K_h(\partial \Theta/\partial z), \tag{9}$$

$$\overline{wq} = -K_h(\partial Q/\partial z), \tag{10}$$

$$\overline{w(E' + p'/\rho)} = -2.0K_m\partial E/\partial z, \tag{11}$$

where K_m and K_h are the eddy coefficients for momentum and heat, respectively. A similar relationship was proposed by Mellor and Yamada (1977) in their level-

2.5 turbulence parameterization, with different formulae for K_m and K_h. Here, following Deardorff (1980), we assume that the eddy coefficients are

$$K_m = 0.1l\sqrt{E}, \tag{12}$$

$$K_h = \begin{cases} K_m & \text{for stable stratification} \\ 3.0K_m & \text{for unstable stratification,} \end{cases} \tag{13}$$

where l is the length scale of the eddies. The length scale for the stable stratification is assumed to be

$$l = \begin{cases} 0.76\{E/[(g/\Theta)(\partial\Theta/\partial z)]\}^{1/2} & \text{if } l < \Delta z \\ \Delta z & \text{otherwise.} \end{cases} \tag{14}$$

As discussed in section 1, we are more interested in the ensemble average than in the subgrid-scale average in this study. Hence, in the unstable layer, Deardorff's length scale is replaced by 0.25 of the observational peak wavelength for the vertical velocity component derived by Caughey and Palmer (1979); that is,

$$l = 0.25\{1.8Z_i[1 - \exp(-4z/Z_i) - 0.0003\exp(8z/Z_i)]\} \tag{15}$$

where Z_i is the height of the inversion, and z is the height above the ground surface. The coefficient 0.25 is introduced in this equation by comparing the dissipation rate and production terms in the turbulent kinetic-energy equation (6) with the same equations in Mellor and Yamada (1974) and Enger (1983a). In order to have a smooth curve of l across the inversion, the length scales of the first three levels above the inversion are artificially set to be $0.5l_i$, $0.125l_i$ and $0.031l_i$, respectively (where l_i is the length scale at the inversion), since vigorous gravity waves can be excited near the inversion by the strong convection in the mixed layer (Kuo and Sun, 1976). A smooth and continuous curve of l across the inversion was also used by Sun and Ogura (1980). The values of l at the remaining levels for stable stratification follow (14). The typical values of l within the convective layer are between 100 and 600 m. Since the small-scale structure of turbulence at large Reynolds number is always approximately isotropic, we use Mellor and Yamada's simple equation for dissipation:

$$\epsilon = CE^{3/2}/l, \tag{16}$$

where we set $C = 0.41$ from comparison of Deardorff's (1980) dissipation coefficient with that of Yamada and Mellor (1975).

3. Initial and boundary conditions

At the upper boundary, all turbulence fluxes and the wind shear are set to zero. The temperature and moisture are fixed. In the surface layer, the similarity equations (Businger et al., 1971) are employed.

The heat fluxes at the ground surface ($-u_*\theta_*$) during the daytime are prescribed as a function of time. Since the Wangara data do not include the surface temperature, the surface heat flux is assumed to be a sinusoidal function with a peak value of 21.6 K cm s^{-1} at 1300 EST and a half-period of 11 h. This value was used by Wyngaard and Coté (1974) and Sun and Ogura (1980). The moisture flux at the ground surface ($-u_*q_*$) is obtained from similarity equations applied to the measured value of the moisture at z_m (z_m = 1.2 m) and the calculated value at the first level z_1, which is 25 m. The shearing stresses ($\overline{uw}$, $\overline{vw}$) at the surface layer can be expressed as

$$\overline{uw} = -K_m\partial U/\partial z = -u_*^2 U_1/(U_1^2 + V_1^2)^{1/2}, \tag{17}$$

$$\overline{vw} = -K_m\partial V/\partial z = -u_*^2 V_1/(U_1^2 + V_1^2)^{1/2}, \tag{18}$$

where U_1 and V_1 are the wind components at z_1.

Data from the Wangara observation at 0900 EST (local time) on day 33 (16 August 1967) were used as the initial conditions for this model. This particular time was chosen partly to facilitate a direct comparison of the numerical results obtained by Deardorff (1974a,b), Wyngaard and Coté (1974), Yamada and Mellor (1975), André et al. (1978), Sun and Ogura (1980) and others. In the model, E = 0.006 m^2 s^{-2} is used as the initial condition for the turbulent kinetic energy. It is found that the initial value of E was not important, since it increased very rapidly in the mixed layer until the dissipation rate could balance the buoyant production term.

The surface geostrophic wind (U_{g0}, V_{g0}) and the thermal winds from the surface to 1 km height and from 1 to 2 km were collected twice per day. Following Yamada and Mellor (1975), parabolic profiles are fitted to these values so that the eastward geostrophic wind component, for example, is given by the following expression:

$$U_g(t,z) = [(\Delta U_g)_2 - (\Delta U_g)_1]z^2/(2\times 10^6) + [3(\Delta U_g)_1 - (\Delta U_g)_2]z/(2\times 10^3) + U_{g0}(t), \tag{19}$$

where $(\Delta U_g)_1$ and $(\Delta U_g)_2$ are the reported thermal winds differences from the surface to 1 km and from 1 to 2 km, respectively. The values for $(\Delta U_g)_1$ and $(\Delta U_g)_2$ at any time between observations are linearly interpolated.

Twenty-two grid points are used in the z direction for the first moments, with a total depth of 2000 m. The staggered grids are used with the first moments defined at 25, 100, 200, . . . , 2000 m and the second moments defined at 50, 150, 250, . . . , 2050 m. The finite difference scheme, trapezoidal in time and centered in space, is chosen in this study.

4. Results and discussion

a. Virtual potential temperature and heat flux

Figures 1 and 2 show the time evolution of the computed mean virtual potential temperature and the heat

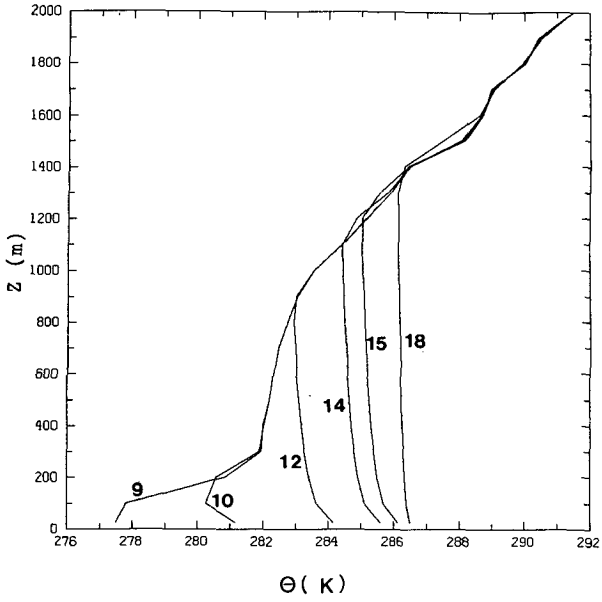

FIG. 1. Calculated profiles of the mean virtual potential temperature during day 33 of the Wangara experiment.

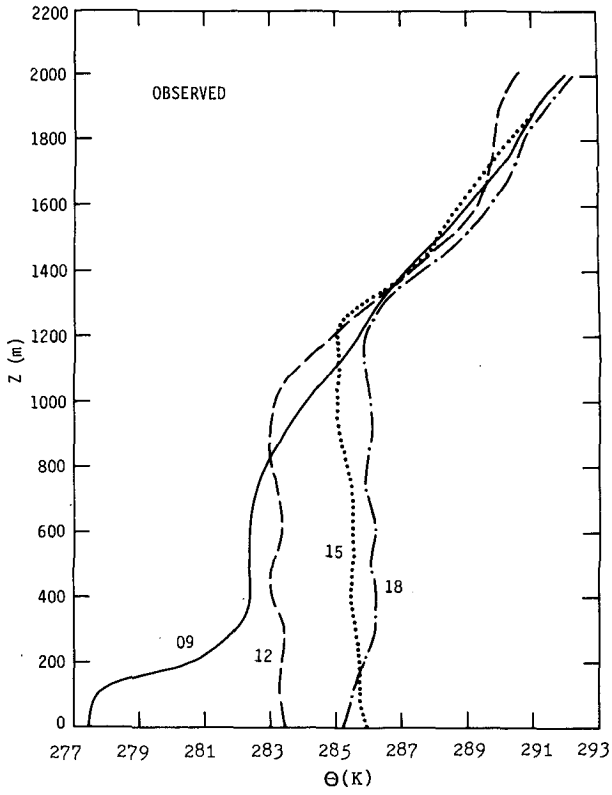

FIG. 3. As in Fig. 1 but observed profiles.

flux, respectively. The observed potential-temperature profiles in Fig. 3 are well simulated during the daytime of day 33. Although a slightly unstable stratification is obtained in the middle of the mixed layer due to calculating the heat flux by (9), this model has reproduced a shallow superadiabatic layer near the ground surface, a deep well-mixed layer in the middle, and an inversion layer atop as observations. These profiles are also generally in good agreement with the numerical simulations of Deardorff (1974a), André et al. (1978) and Sun and Ogura (1980). Also, the simulated depth of the mixed layer is comparable to that observed. Radiative transfer is included in Deardorff's model, but not in this study. A comparison of these numerical results indicates that radiation does not contribute significantly to the temporal evolution of the temperature field during the daytime when the convective transport process dominates. Radiation was also ignored by Wyngaard and Coté (1974), Sun and Ogura (1980) and Enger (1983a).

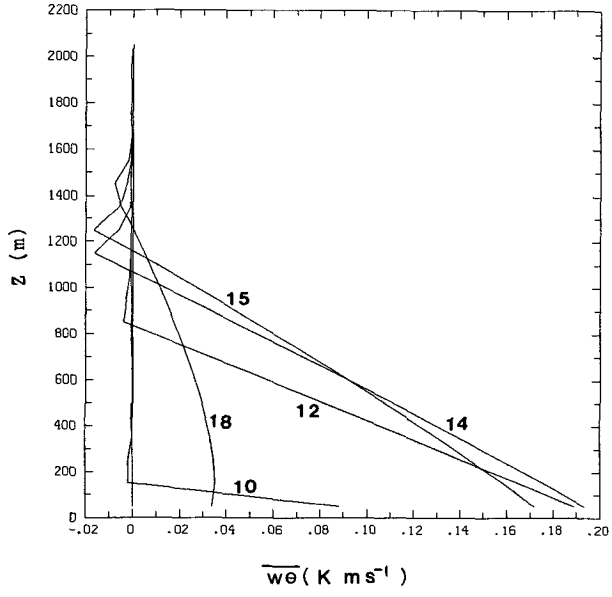

FIG. 2. Calculated profiles of the vertical heat flux.

As mentioned in the Introduction, a set of prognostic equations was used to calculate the fluxes of heat and moisture by Wyngaard and Coté (1974), as well as Sun and Ogura (1980), in contrast to the use of a very simple Eq. (9) here. It is also noted that the surface heat fluxes in this model are identical to those used by Wyngaard and Coté (1974) and Sun and Ogura (1980). In this respect, it is interesting to compare those results with the findings we have obtained. Figure 2 shows that the calculated vertical heat flux in a convective layer is a linear function of height, becoming slightly negative near the inversion. The downward heat flux at the inversion is about 4 to 9% of the upward surface heat flux during the period of strong convection. This agrees well with the 5 to 12% simulated by Wyngaard and

Coté (1974) and the 4 to 7% by Sun and Ogura (1981). Ratios in other references vary, including 5% observed in the atmosphere by Lenschow (1970, 1974), 14 to 21% in Deardorff's (1974a) three-dimensional simulation, less than 2% in Yamada and Mellor (1975), 9 to 20% in Zeman and Lumley (1976) and 5 to 8% obtained by Willis and Deardorff (1974) in their laboratory experiments. Thus, the calculated heat flux is consistent with many earlier calculations and measurements.

b. Moisture and moisture flux

The surface flux of moisture in our model is calculated from the value at z_m (=1.2 m) and the calculated value at the height of 25 m. The value at z_m is calculated by linear interpolation between the measured values at the two observational periods. The calculated humidity profiles shown in Fig. 4 indicate that the mixing ratio decreases only slightly with height in the mixed layer due to strong convection. This is consistent with the observational data (see Fig. 5) and numerical simulations (Deardorff, 1974a; Sun and Ogura, 1980), as well as other observations (Wyngaard *et al.* 1978; Warner and Telford, 1967). It is noted that the Wangara data (Fig. 5) show a rather rapid decrease of humidity with time on the morning of day 33, a feature captured by the present model but not well simulated by either Wyngaard and Coté (1974) or by Sun and Ogura (1980) due to the larger surface moisture flux applied in their models.

The profiles of the moisture flux presented in Fig. 6 are similar to those obtained by Deardorff (1974a), Wyngaard and Coté (1974) and Sun and Ogura (1980). As the mixed layer grows, the surface moisture supply is insufficient to maintain the early morning mixing ratio near the ground, and both the calculated and observed values decrease with time.

A physically unrealistic downward moisture flux, which developed near the inversion in the models of Deardorff (1974a), Wyngaard and Coté (1974) and

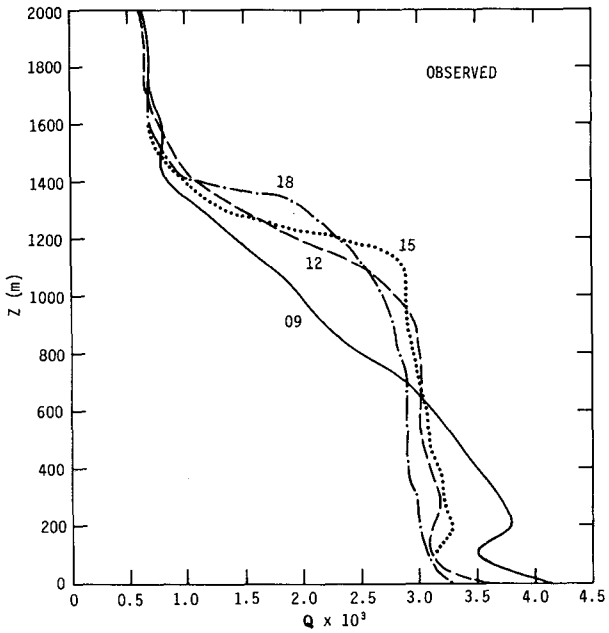

FIG. 5. As in Fig. 4 but observed profiles.

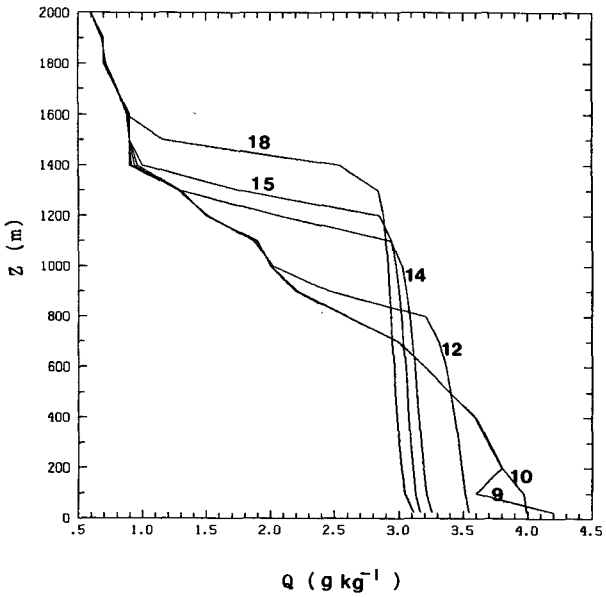

FIG. 4. Calculated profiles of the mean mixing ratio.

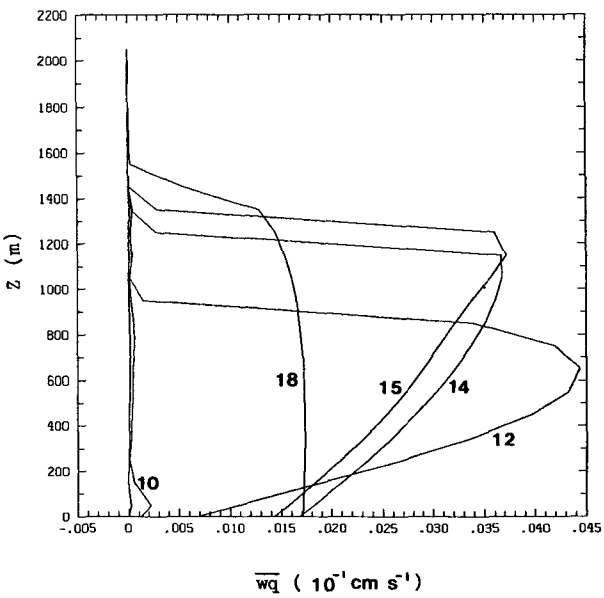

FIG. 6. Calculated profiles of the vertical moisture flux.

André et al. (1978), does not appear in this model or in Sun and Ogura (1980). When a cool and moist air parcel penetrates into the overlying stable layer from below, a dry and warm air parcel in the stable layer will move into the mixed layer to compensate. Thus, the heat flux in the inversion should be downward, but the moisture flux upward. This may also be related to the fact that while the observed potential temperature is nearly neutral to even slightly stable, the humidity decreases slightly with height.

c. *Wind and momentum fluxes*

The calculated x- and y-components of the mean wind are presented in Figs. 7 and 8, respectively. The overall agreement is good compared to the numerical simulations of Yamada and Mellor (1975) and those of André et al. (1978). But the computed mean wind is only fair compared to the observed mean wind profiles shown in Figs. 9 and 10. The computed U is close to the observation until 1500 EST. At 1800 EST, the computed U is about -5.5 m s^{-1} in the mixed layer, which is also comparable to the observation. However, the model minimum value of $U = -5$ m s^{-1} occurs at the height of 1700 m, but the observational value is only about -3.5 m s^{-1} at this height. It is also noted that in the mixed layer the observed wind is not so well mixed as the computed wind. This discrepancy has also appeared in other models (Deardorff, 1974a; André et al., 1978; Sun and Ogura, 1980). The magnitude of the computed V is also larger than that observed in the late afternoon. At 1800 EST, the calculated y-component wind speed is about 3.5 m s^{-1} in the mixed layer (the same value was obtained by Yamada and Mellor, 1975), in contrast to the observed value of 1.6 m s^{-1}. This discrepancy may be caused by using an inaccurate geostrophic wind in the momen-

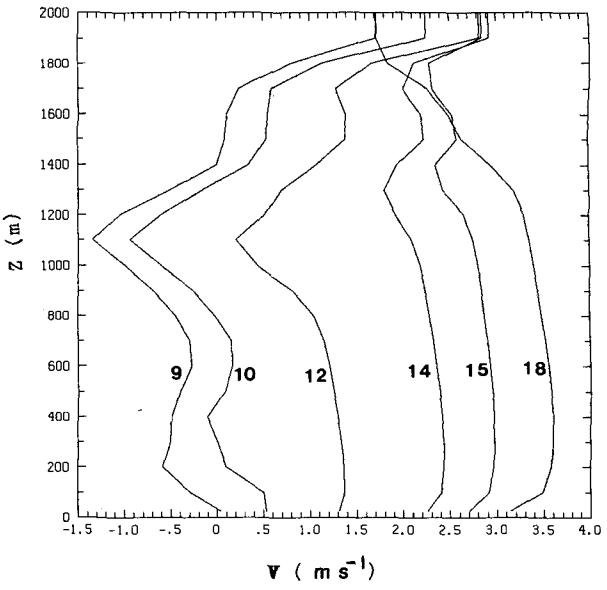

FIG. 8. Calculated profiles of the y-component mean wind.

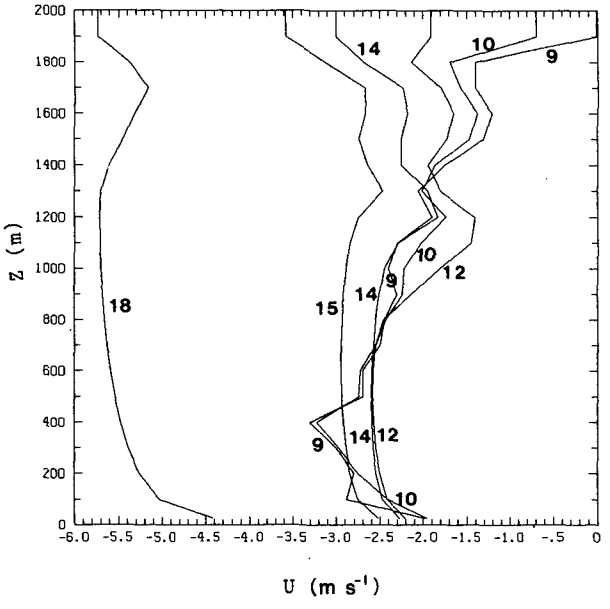

FIG. 7. Calculated profiles of the x-component mean wind.

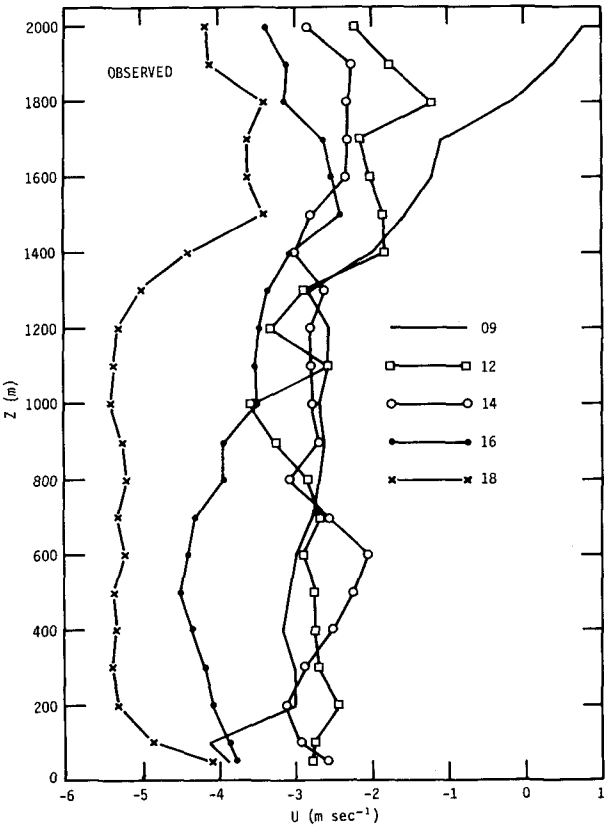

FIG. 9. As in Fig. 7 but observed profiles.

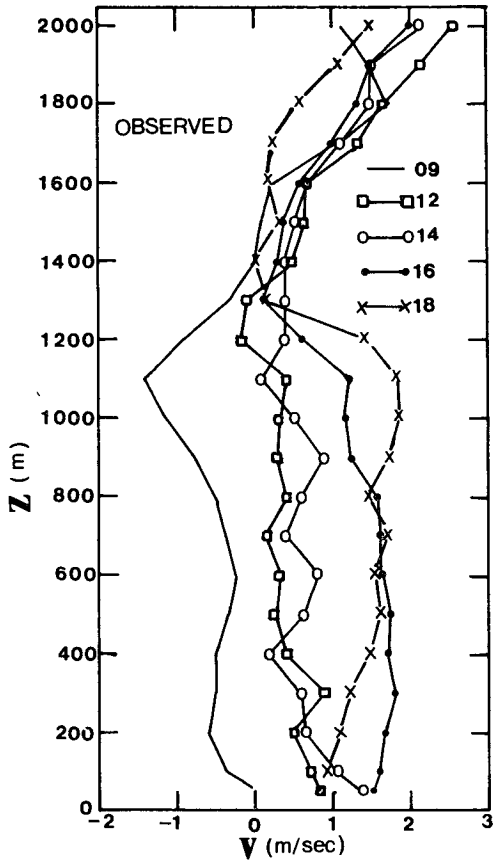

FIG. 10. As in Fig. 8 but observed profiles.

tum equation or by not treating the momentum fluxes appropriately. The difficulty in simulating the observed wind has also been encountered in Deardorff's (1974a) three-dimensional model and other models. The profiles of the simulated turbulent fluxes of momentum (not shown) are similar to those of André et al. (1978), but our surface stress is larger than theirs. The difference may come from a larger roughness length being applied in our model.

d. Turbulent kinetic energy

It is well recognized that the scaling proposed by Deardorff (1970) can produce universal profiles of turbulence parameters in the convective boundary layer. This study follows his arguments in prescribing scaling factors for the following quantities: the depth of the mixed layer Z_i and the convective velocity $w_* = [g(-u_*\theta_*)Z_i/\Theta]^{1/3}$, where $\Theta = 273$. The calculated, dimensionless, turbulent kinetic energy is presented by the dashed–double dotted line in Fig. 11. Enger (1983a) proposed that the turbulent kinetic energy observed during the Ashchurch (Caughey and Palmer, 1979) and Minnesota (Izumi and Caughey, 1976) experiments can be summarized by the following equation:

$$E/w_*^2 = 0.5\{0.62 + 1.8(z/Z_i)^{2/3} - 1.65(z/Z_i)^{4/3}\}. \quad (20)$$

This equation is shown by a solid line in Fig. 11. The same figure also includes the laboratory experimental data by Willis and Deardorff (1974) (dashed line), the numerical simulation by André et al. (1978) (dashed–dotted line), and the numerical simulation by Enger (1983a) (dotted line). The value of E/w_*^2 that we obtained at 1500 EST is close to the observational value for $z/Z_i < 0.5$. The calculated maximum of about 0.56 occurred at the height of $z/Z_i \approx 0.3$, while the observed maximum of 0.55 occurred at the height of $z/Z_i \approx 0.4$. The calculated value, however, departs from the observations and approaches the laboratory experimental data in the upper mixed layer. The observed value from the field experiments is 0.3, while it is only about 0.2 from the laboratory experiments at the inversion layer. Enger's result seems very close to the observations for $0.1 < z/Z_i < 0.5$, but his value of E/w_*^2 is about 0.1 larger than that observed near the ground surface. Enger's result also departs from the observational value and approaches the value of the experimental data in the upper mixed layer. The value of E/w_*^2 obtained by André et al. is about 0.15 smaller than the observations in the entire mixed layer. From this diagram we can see that our turbulent kinetic energy seems acceptable compared to other numerical

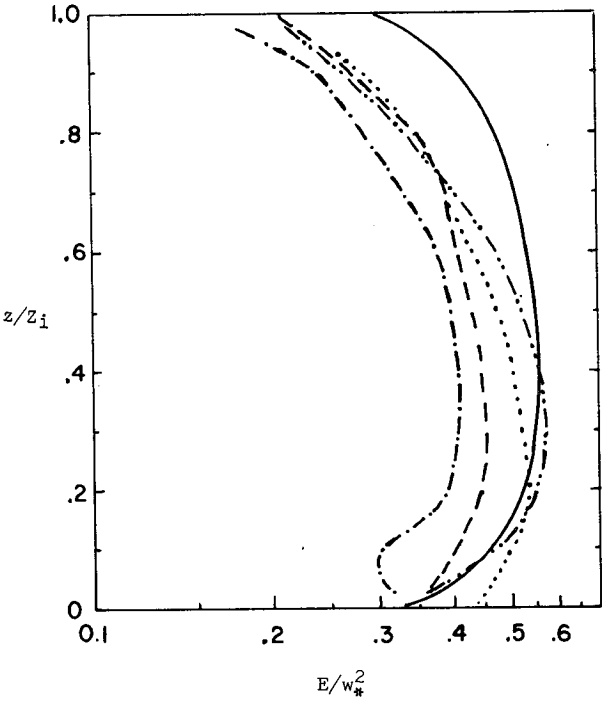

FIG. 11. The dimensionless turbulent kinetic energy (E/w_*^2). Equation (20) is presented by a solid line, Willis and Deardorff's laboratory experiment by a dashed line, André et al.'s by a dashed–dotted–line, Enger's by a dotted line, and the present model by a dashed–double dotted line.

results and observations. It is also noted that the turbulent kinetic energies obtained by Yamada and Mellor (1975), as well as Sun and Ogura (1980), are too small compared to observations near the ground surface (Sun and Ogura, 1980) due to an inappropriate similarity equation.

The budget of the turbulent kinetic energy computed from our model at 1500 EST, shown in Fig. 12, is close to that obtained by André et al. (1978) and Sun and Ogura (1980). The dissipation rate, ϵ, and the buoyant production rate, B, are the dominant terms, nearly compensating each other except near the surface and near the inversion. The transport term, T, becomes important near the inversion, because the turbulence near the inversion is sustained by the transport term against the dissipation and the negative buoyant production. The transport term at the inversion is 17% of the heat flux at ground surface according to Fig. 12, which is close to the value of 20% obtained by Sun and Ogura (1980) and the 23% obtained by André et al. (1978), but is much larger than the value of 3% obtained by Yamada and Mellor (1975). The turbulent transport is also important in the lower mixed layer in this and other models.

As mentioned previously, the turbulent kinetic energy in the upper mixed layer in this model is smaller than that observed. Several factors may have caused this discrepancy. First, a single length scale associated with the vertical velocity is used in this model instead of the multiple length scales, which are appropriate for a real atmosphere. Second, the eddy coefficient of this model may still be too small or dissipation may be too large in the upper mixed layer. It may also be caused by the eddy-coefficient relations used in (7)–(10), which have been criticized by André et al. (1976a,b), Zeman and Lumley (1976), Sun and Ogura (1980) and others. Weak turbulences in the upper mixed layer may also affect the concentration distribution of pollutants there, which will be discussed in Part II of this study. Further study is required to solve this problem, because this discrepancy also exists in the third-order closure model developed by André et al. (1978). However, in comparison to observations, our computed wind, temperature, moisture and turbulent kinetic energy seem as good as those obtained by Wyngaard and Coté (1974), Yamada and Mellor (1975), André et al. (1978), Sun and Ogura (1980) and other higher-order turbulence schemes.

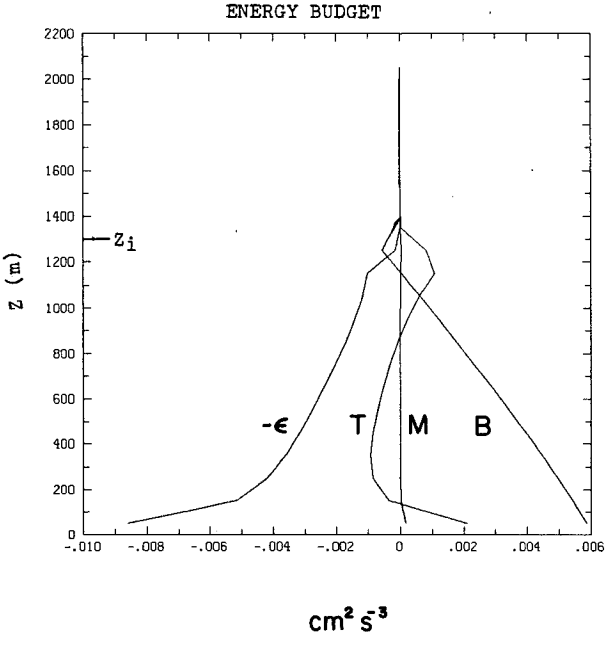

FIG. 12. Calculated turbulent kinetic energy budget at 1500 EST. Here B is buoyant production, M mechanical (shear) production, $-\epsilon$ dissipation, and T turbulent transport.

5. Summary

An ensemble average turbulence model for a moist convective planetary boundary layer was developed in this paper. In addition to the four prognostic equations for virtual potential temperature, mixing ratio, and x- and y-components of wind, this model requires a prognostic equation to calculate the turbulent kinetic energy, which is used to specify the eddy coefficients following Deardorff (1980). The observation length scale associated with the vertical velocity is used in the mixed layer, while the length scale associated with internal gravity waves is applied in the overlying stably stratified atmosphere. The observational wind, moisture and temperature in the Wangara experiment have been well simulated by this simple model. Furthermore, some of the second moments also agree well with those obtained by other more sophisticated models and observations.

The parameterization is accurate but simple enough to be incorporated into a pollution model, as well as a three-dimensional mesoscale model being developed at Purdue University.

Acknowledgments. The authors wish to thank the reviewers and Mr. P. Haines at Purdue University for reading the draft and providing very useful comments. Part of this work was supported by the National Science Foundation under Grant ATM-821965 by the Global Atmospheric Research Program and ATM-8313418 by the Meteorology Program. Part of the numerical computation was done at the National Center for Atmospheric Research, which is supported by the National Science Foundation.

REFERENCES

André, J. C., G. DeMoor, P. Lacarrere and R. duVachat, 1976a: Turbulence approximation for inhomogeneous flow. Part I: The clipping approximation. *J. Atmos. Sci.*, **33**, 476–481.

——, ——, —— and ——, 1976b: Turbulence approximation for inhomogeneous flow. Part II: The numerical simulation of a penetrative convection experiment. *J. Atmos. Sci.*, **33,** 482–491.
——, ——, ——, G. Therry and R. duVachat, 1978: Modeling the 24 hour evolution of the mean and turbulent structures of the planetary boundary layer. *J. Atmos. Sci.*, **35,** 1861–1883.
Businger, J. A., J. C. Wyngaard, Y. Izumi and E. F. Bradley, 1971: Flux-profile relationships in the atmospheric surface layer. *J. Atmos. Sci.*, **28,** 181–189.
Caughey, S. J., and S. G. Palmer, 1979: Some aspects of turbulence structure through the depth of the convective layer. *Quart. J. Roy. Meteor. Soc.*, **105,** 811–827.
Clark, R. H., D. G. Reid and A. J. Troup, 1971: The Wangara experiment: Boundary layer data. Tech. Pap. 19., Div. Meteor. Phys., CSIRO, 340 pp.
Deardorff, J. W., 1970: Convective velocity and temperature scales for the unstable planetary boundary and for Rayleigh convection. *J. Atmos. Sci.*, **27,** 1211–1213.
——, 1974a: Three-dimensional numerical study of the height and mean structure of a heated planetary boundary layer. *Bound.-Layer Meteor.*, **7,** 81–106.
——, 1974b: Three-dimensional numerical study of turbulence in an entraining mixed layer. *Bound.-Layer Meteor.*, **7,** 199–226.
——, 1980: Stratocumulus-capped mixed layers derived from a three-dimensional model. *Bound.-Layer Meteor.*, **18,** 495–527.
Enger, L., 1983a: Numerical boundary layer modeling with application to diffusion. Part I: A two dimensional higher order closure model. Rep. No. 70, Dept. of Meteorology, University of Uppsala, 54 pp.
——, 1983b: Numerical boundary layer modeling with application to diffusion. Part II: A higher order closure dispersion model. Rep. No. 71, Dept. of Meteorology, University of Uppsala, 45 pp.
Izumi, Y., and S. J. Caughey, 1976: Minnesota 1973 atmospheric boundary layer experiment data report. AFGL Environment Res. Pap. No. 547, AFGL, 28 pp.
Kaimal, J., J. C. Wyngaard, P. A. Haugen, O. R. Coté, Y. Izumi, S. J. Caughey and C. J. Readings, 1976: Turbulence structure in the convective boundary layer. *J. Atmos. Sci.*, **33,** 21–40.
Kuo, H. L., and W.-Y. Sun, 1976: Convection in the lower atmosphere and its effects. *J. Atmos. Sci.*, **33,** 21–40.
Lenschow, D. W., 1970: Airplane measurements of planetary boundary layer structure. *J. Appl. Meteor.*, **9,** 874–884.
——, 1974: Model of the height variation of the turbulent kinetic energy budget in the unstable planetary boundary layer. *J. Atmos. Sci.*, **31,** 465–474.
Mellor, G. L., and T. Yamada, 1974: A hierarchy of turbulence closure models for planetary boundary layers. *J. Atmos. Sci.*, **31,** 1791–1806.
——, and ——, 1977: A turbulence model applied to geophysical fluid problems. *Proc. Symp. on Turbulent Shear Flows.* Pennsylvania State University, 1–14.
Sun, W.-Y., and Y. Ogura, 1980: Modeling the evolution of the convection planetary boundary layer. *J. Atmos. Sci.*, **37,** 1558–1572.
——, and W.-R. Hsu, 1985: Numerical simulation of atmospheric mesoscale convection. *Supercomputer Applications,* R. W. Numrich, Ed., Plenum, 145–158.
——, and C.-Z. Chang, 1986: Diffusion model for a convective layer. Part II: Plume released from a continuous point source. *J. Climate Appl. Meteor.*, **25,** 1454–1463.
Warner, J., and J. W. Telford, 1967: Convection below cloud base. *J. Atmos. Sci.*, **24,** 371–382.
Willis, G. E., and J. W. Deardorff, 1974: A laboratory model of the unstable planetary boundary layer. *J. Atmos. Sci.*, **30,** 558–567.
Wyngaard, J. E., and O. R. Coté, 1974: The evolution of the convective planetary boundary layer—a higher-order closure model study. *Bound.-Layer Meteor.*, **7,** 289–308.
——, W. T. Pennell, D. H. Lenschow and M. A. LeMone, 1978: The temperature-humidity covariance budget in the convective boundary layer. *J. Atmos. Sci.*, **35,** 47–58.
Yamada, T., and G. L. Mellor, 1975: A simulation of the Wangara atmospheric boundary layer data. *J. Atmos. Sci.*, **32,** 2309–2329.
Zeman, O., and J. L. Lumley, 1976: Modeling buoyancy-driven mixed layers. *J. Atmos. Sci.*, **33,** 1974–1988.